Absorbed dose analysis of dental cone-beam computed tomography using Monte Carlo simulations

Jinwoo Kim [a], Bitbyeol Kim [a], Ho Kyung Kim [a,b*]
[a]*School of Mechanical Engineering, Pusan National University, Busan 46241, Republic of Korea*
[b]*Center for Advanced Medical Engineering, Pusan National University, Busan 46241, Republic of Korea*
[*]*Corresponding author: hokyung@pusan.ac.kr*

1. Introduction

Because the exposure to cumulative computed tomography (CT) scans can cause significant harm to the patient, there has been an increasing interest in radiation exposure during CT scans [1]. In contrast, dental cone-beam CT (CBCT) has been used indiscriminately because the effective dose in the dental CBCT is relatively lower than that in the multislice CT [2-4].

Since, on the other hand, the safety of low-dose radiation is not clearly known [5], efforts should be made to reduce the patient dose. In order to minimize the patient dose, accurate dose estimation is important.

In dental CBCT imaging, dose estimation should be performed according to the oral structure of the patient [6]. However, it is impossible to estimate accurately the patient-specific dose using the experimental methods such as conventional CT dose index or anthropomorphic phantoms [2,6].

The purpose of this study is to analyze the dose distribution for typical dental CBCT scanning protocol using the Monte Carlo (MC) method to propose an optimal scan protocol that minimizes patient dose while maintaining image quality.

2. Materials and Methods

MC simulations using the Monte Carlo N-Particle transport code (MCNP version 5, RSICC, Oak Ridge, TN, USA) were performed for anthropomorphic phantom (XCAT version 2.0, Duke University, Durham, NC, USA), as shown in Fig. 1.

The head and neck part of XCAT phantom was created in 140x140x125 voxels with voxel pitch of 2 mm. Originally, the head and neck part of XCAT phantom was composed of 12 materials, but it was reduced to 7 materials for efficient simulation. The total number of histories of the MC simulation was 360 million.

The imaging protocol used for the MC simulations was the typical dentoalveolar imaging. The x-ray source was a cone-shaped beam with a field-of-view of 12x8 cm, irradiated the phantom in a step angle of 0.4 degree while rotating 360 degrees. The x-ray spectrum was the 88 kVp and the total filtration was 3.0 mm Al. The source-to-object distance and the source-to-detector distance were 430 and 600 mm, respectively.

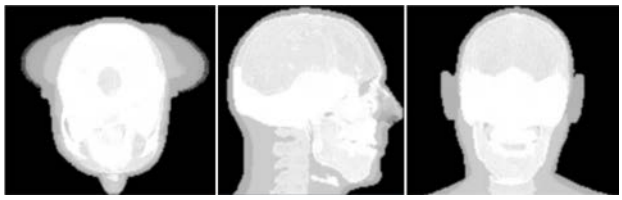

Figure 1. Phantom used for Monte Carlo simulations: head and neck part of XCAT phantom.

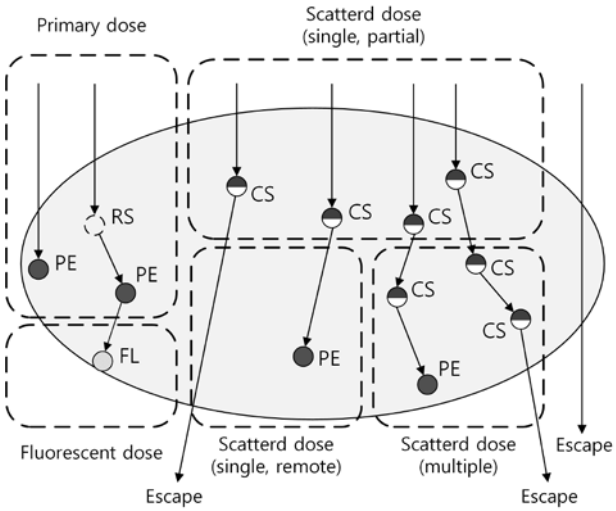

Figure 2. Classification of primary and scattered dose in this study. PE, CS, RS, and FL denote the photoelectric absorption, Compton scattering, Rayleigh scattering, and x-ray fluorescence, respectively.

To calculate the dose distribution from the MC simulation results, a list-mode analysis was performed. All particle data tracked during the MC simulation such as interaction type, location, and absorbed energy were classified according to the type of x-ray interaction as shown in Fig. 2, and the energy absorbed by each interaction was calculated.

As shown in Fig. 2, Compton scattering deposits some energy at the point where the scattering event occurs and changes the direction of propagation. Then the scattered photons interact with the material at other points until all energy is lost. Thus, the scattered x-ray photons are classified into the single and multiple scattered photons to analyze the contributions of dose due to single scattered photons and multiple scattered photons in total dose, separately.

3. Preliminary Results

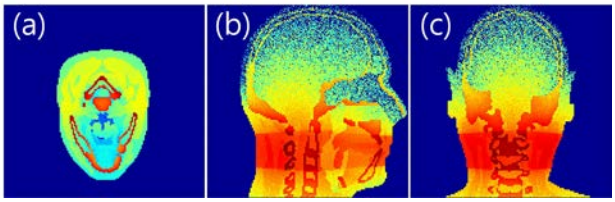

Figure 3. Absorbed energy distribution of XCAT phantom. (a), (b), and (c) show the axial, sagittal, and coronal planes of the phantom, respectively.

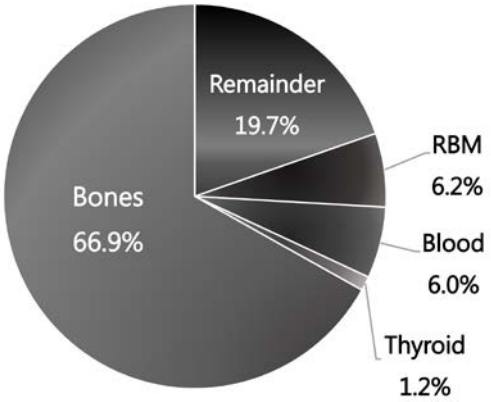

Figure 4. Contribution of organs to absorbed dose (total 0.177 fGy/particle). RBM denotes red bone marrow.

Figure 3 shows the absorbed energy distributions at each cross-section of the XCAT phantom. The calculated results are normalized by the total number of histories of the MC simulation, and the closer the color of the graph to the red, the higher the absorbed energy.

Figures 4 and 5 show the organ-wise absorbed dose and the contribution of single scattered, multiple scattered, and primary photons to the total absorbed dose.

4. Conclusions

The calculation of the absorbed dose distributions due to dental CBCT imaging was performed using an anthropomorphic phantom.

As shown in Fig. 4, higher doses were delivered to bones than other tissues. Since bones have a relatively higher x-ray attenuation coefficient than tissues, more x-ray interactions would have occurred and thus higher doses were delivered.

As shown in Fig. 5, the proportion contributing to total dose was higher in the scattered dose than in the primary dose. This is because the dose due to photoelectric absorption after scattering events is included in the scattered dose and the Compton scattering was more dominant than photoelectric absorption in soft tissues, which constitute the majority of the human body. The fluorescent dose was almost negligible.

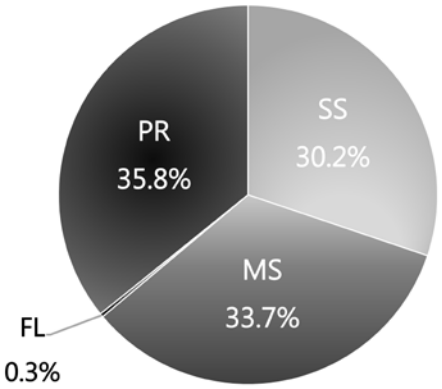

Figure 5. Contribution of each dose classified to absorbed dose. PR, SS, MS, and FL denote primary dose, single scattered dose, and multiple scattered dose, fluorescent dose, respectively.

The important further study is the validation of the results with the experimental measurements.

ACKNOWLEDGEMENT

This work was supported by the National Research Foundation of Korea (NRF) grants funded by the Korea governments (MSIP) (No. 2013M2A2A904613 and No. 2014R1A2A2A01004416).

REFERENCES

[1] D. J. Brenner and E. J. Hall, “Computed tomography – An increasing source of radiation exposure,” New Engl. J. Med. **357**(22), pp. 2277-2284, 2007.
[2] Ruben Pauwels et al, “Effective dose range for dental cone beam computed tomography scanners,” Eur. J. Radiol. **81**, pp. 267-271, 2012.
[3] J. B. Ludlow et al, “Dosimetry of two extraoral direct digital imaging devices: NewTom cone beam CT and Orthophos Plus DS panoramic unit,” Dento. Radiol. **32**, pp. 229-234, 2003.
[4] G. Brix et al, “Assessment of a theoretical formalism for dose estimation in CT: an anthropomorphic phantom study,” Eur. Radiol. **14**, pp. 1275-1284, 2004.
[5] D. J. Brenner et al, “Cancer risks attributable to low doses of ionizing radiation: Assesing what we really know,” PNAS **100**(24), pp. 13761-13766, 2003.
[6] C. H. McCollough et al, “CT dose index and patient dose: they are not the same thing,” Radiol. **259**(2), pp. 311-316, 2011.